Remarkable changes in the near-infrared spectrum of the nova-like variable V4332 Sgr

Dipankar P.K. Banerjee

Physical Research Laboratory, Navrangpura, Ahmedabad, India, 380009

orion@prl.ernet.in

Watson P. Varricatt

Joint Astronomy Center, 660 N. Aohoku Place, Hilo, Hawaii-96720, USA

w.varricatt@jach.hawaii.edu

Nagarhalli M. Ashok

Physical Research Laboratory, Navrangpura, Ahmedabad, India, 380009

ashok@prl.ernet.in

and

Olli Launila

SCFAB-KTH, Atomic and Molecular Physics, Roslagstullsbacken 21, SE-106 91, Stockholm, Sweden

olli@physics.kth.se

ABSTRACT

We report on recent near-IR observations of V4332 Sgr - the nova-like variable that erupted in 1994. Its rapid, post-outburst evolution to a cool M type giant/supergiant, soon after its outburst, had showed that it was an unusual object differing from other eruptive variables like classical/symbiotic novae or born-again AGB stars. The present study of V4332 Sgr was motivated by the keen interest in the recent eruption of V838 Mon - an object with a spectacular light-echo and which, along with V4332 Sgr, is believed to belong to a new class of objects (we propose they may be called "quasi-novae"). Our observations show new developments in the evolution of V4332 Sgr. The most striking feature is the detection of several molecular bands of AlO - a rarely seen molecule

in astronomical spectra - in the JHK spectra. Many of these bands are being detected for the first time. The only other detection of some of these AlO bands are in V838 Mon, thereby showing further spectral similarities between the two objects. JHK photometry shows the development of a new dust shell around V4332 Sgr with a temperature of $\sim$ 900K and a lower limit on the derived mass of $M_{\rm dust} = 3.7 \times 10^{-12} M_{\odot}$. This dust shell does not appear to be associated with ejecta of the 1994 outburst but is due to a second mass-loss episode which is not expected in a classical nova outburst. The cold molecular environment, suggested by the AlO emission, is also not expected in novae ejecta. We model the AlO bands and also discuss the possible formation mechanism of the AlO. These results show the need to monitor V4332 Sgr regularly - for unexpected developments. The results can also be significant in suggesting possible changes in the future evolution of V838 Mon.

Subject headings: Stars: individual: V4332 Sgr - Infrared: stars - Stars: novae - Techniques: spectroscopic

1. Introduction

V4332 Sagittarii (V4332 Sgr) erupted in a nova-like outburst in February, 1994. The light curve of the object (Martini et al., 1999) showed a slow rise in brightness from an estimated, pre-outburst magnitude of $B \sim 18$ to an extended period of maximum brightness with $V = 8.5$. The only detailed study of the object by Martini et al. (1999) showed that its outburst does not conform to known categories of eruptive variables. V4332 Sgr showed a rapid cooling over three months - from 4400 to 2300K - and evolved into a cool M giant/supergiant. A similar behaviour has also been observed in the recent (January 2002) outburst of V838 Monocerotis. It appears, that V838 Mon and V4332 Sgr are analogues and together may be defining a new class of objects (Munari et al. 2002; Bond et al. 2003). A third, possible member of this class is a red variable that erupted in M31 called M31 RV (Rich et al. 1989). While the outburst mechanism of such objects is not well understood, a recent result by Soker and Tylenda (2003) explains the outburst as a merger event between two stars - the release of gravitational energy leading to the the nova-like outburst. This is in distinct contrast to the classical nova scenario wherein a thermo-nuclear runaway on the surface of the white dwarf, accreting matter from its secondary companion, leads to the nova eruption. The limited studies on V4332 Sgr (with none in the IR) - and also the current interest in V838 Mon - prompted us to make the present observations of V4332 Sgr to see how it had evolved with time. These observations, which give interesting results, are

reported here.

2. Observations

Spectroscopic observations were done with the 3.8m United Kingdom IR Telescope (UKIRT), Hawaii and the 1-5 micron Imager Spectrometer (UIST) using a 1024×1024 InSb array. Observations were done by nodding the telescope on two positions separated by 12″ along a 4 pixel (0.48″) wide slit. Flat fielding was done with a black body mounted inside the instrument and spectral calibration was done using an Argon lamp. Spectra of the source in the J, H and K bands were obtained on 2003 April 24. A second J band spectrum was obtained on 2003 May 4. Table 1 gives the details of the spectroscopic observations. Because of possible slit-losses, we have calibrated the spectra using the photometry of 2003 June 19 assuming constancy in source brightness over the 56 day gap between the spectroscopic and photometric observations. The UKIRT photometric observations were done using UFTI (UKIRT Fast-Track Imager) which uses a 1024×1024 HgCdTe array and gives a plate scale of 0.091″/pixel. The sky was photometric with a K band seeing of 0.69″. Observations in the JHK bands were done by dithering the object in several positions. Separate dark observations were done and flat field corrections were applied using flat fields generated from the object observations by median combining the observed frames. The UKIRT standard star FS35 was observed under similar conditions and used for flux calibration. The details of the observations and the derived JHK magnitudes are given in Table 2.

3. Results

3.1. JHK spectroscopy

We show in Figure 1 the JHK spectra of V4332 Sgr. The most striking feature of the spectra is the presence of several, strong, molecular bands in emission. Based on laboratory spectra by Launila & Jonnson (1994) we have identified the bands to be due to rotational-vibrational transitions in the $A^2\Pi_i$–$X^2\Sigma^+$ band system of AlO. The $A^2\Pi_i$ state of AlO is a low lying electronic state - the $A^2\Pi_{3/2}$, $A^2\Pi_{1/2}$ states being typically 1 ev above the ground level. To facilitate a comparison between the observed and predicted bands, a synthetic spectrum of AlO (discussed later in more details) is also shown in Figure 1. We have listed in Table 3 the laboratory wavelengths of the different bands whose detection seems to be certain and also marked their positions in Figure 1. The good match between the observed and expected wavelengths makes the identification of the AlO bands secure. At optical

wavelengths the detection of AlO in astronomical objects is rather rare - a notable exception being its detection in the cool, circumstellar environment of the peculiar red giant star U Equulei (Barnbaum et al., 1996). In the near-IR, the only detection of AlO is very recent and is coincidentally seen in an object similar to V4332 Sgr, i.e. V838 Mon (Geballe et al. 2002, Banerjee & Ashok 2002b, Bernstein et al. 2003). There are no published results on the AlO bands in V838 Mon as yet. Further, only some of the AlO bands reported here are seen in V838 Mon viz. - the (1,0) and (4,0) bands - the other bands reported here are new detections.

3.2. Spectral Energy Distribution

The spectral energy distribution (SED) of V4332 Sgr (Figure 2) shows considerable change between 2MASS observations (J = 12.1 , H = 11.6, $K_{\rm s}$ = 10.992; epoch: 18 May 1998) and now. The JHK fluxes in Figure 2 have been computed after reddening corrections adopting $E(B-V)$= 0.32 from Martini et al. (1999) and using zero magnitude fluxes and the standard relations between $A_{\rm V}$, $A_{\rm J}$, $A_{\rm H}$ and $A_{\rm K}$ from Koornneef (1983). A 3250K blackbody curve fits the 2MASS data fairly well. The present data shows a steep rise towards the red. A black-body fit between 900-1000K gives the most reasonable fit to the data though there is some deviation in the J band. It is possible that a hotter black-body component is also present, probably due to some flux from the central star seen in the 2MASS data. A multi-component black-body fit (with temperatures of 900K and 3250K) is also shown which does suggest the presence of a hot component. But to infer anything more on the hot component is difficult from the present data. What is however clear, is the presence of a cool 900-1000K component, which we interpret to arise from a dust shell that has formed subsequent to the 2MASS observations. The luminosity of the dust shell $L_{\rm dust}$ can be found by numerically integrating the 900K SED curve and multipying by $4\pi d^2$ - where d is the distance to V4332 Sgr. Martini et al. (1999) have estimated an upper limit of d = 300pc for V4332 Sgr. For such a value of d, $L_{\rm dust}$ is found to be $\sim 0.85 L_{\odot}$. Since the dust shell is reasonably well approximated by a black-body we equate $L_{\rm dust} = 4\pi {R_{\rm shell}}^2 \sigma {T_{\rm dust}}^4$ and get a shell radius $R_{\rm shell}$ of $\sim 35 R_{\odot}$ (where σ is the Stefan-Boltzmann constant and $T_{\rm dust}$ is the dust temperature). This shell cannot be associated with the ejecta from the 1994 outburst which had an expansion velocity in the range 200-300 km/s (from the Hα line widths of Martini et al. (1999)) and, in the absence of any deceleration, should have a radius of $\sim 10^5 R_{\odot}$ at present. This disagrees too severely with the derived shell radius. The distance d has to be boosted to an unreasonably large value of $\sim$ 1 Mpc (making the object extra-galactic) to have consistency between the derived shell size from luminosity and kinematic arguments. It therefore appears that the matter in the shell is not associated with the 1994 outburst

but involves a second episode of mass-loss. Some additional support for this conclusion is that the angular diameter of the shell from the 1994 outburst, should be $\sim 3.0''$ (for $d =$ 300pc) at present and resolvable in the K band images (Table 2) which taken at $0.69''$ seeing - this is not found to be the case. However, it must be kept in mind, that the ejecta of 1994 may have cooled to a lower temperature than 900K and hence its peak emission will not be in the K band but rather at longer wavelengths. It may be pointed out, that the distance estimate of 300pc by Martini et al (1994), based on the observed spectral class at outburst and derived intrinsic luminosity, may be uncertain to some extent. Thus, a change in d will affect the derived dust-shell luminosity and mass (derived subsequently). However, the main conclusion that the 900K dust shell is not due to the 1994 outburst, should still remain valid. This conclusion - based on comparison of the derived $R_{\rm shell}$ from kinematic and luminosity arguments - should not be affected by any reasonable error in the distance estimate.

The mass of the dust shell can be calculated as $M_{\rm dust}$ =1.1×10^{6} $d^2(\lambda F_\lambda)_{\rm max}$ / ${T_{\rm dust}}^6$ (Woodward et al. 1993). Here $M_{\rm dust}$ is in units of $M_\odot$, $T_{\rm dust}$ is in units of 10^3K, d is in kpc and $(\lambda F_\lambda)_{\rm max}$ is measured at the peak of the SED of the dust in Wcm^{-2}. The dust is assumed to comprise of carbon particles having a size and density of $\leq 1\mu$m and 2.25 gm/cm^3 respectively. By extrapolating the 900K graph of Figure 2 (lower panel) to longer wavelengths to determine $(\lambda F_\lambda)_{\rm max}$, we find $M_{\rm dust} = 3.66 \times 10^{-12} M_\odot$ for T = 900K and d = 300pc. For a canonical value of 200 for the gas-to-dust ratio, the mass of the gas is $M_{\rm gas} = 7.3 \times 10^{-10} M_\odot$. The assumption that carbon particles make up the dust shell, may not be entirely valid since silicates are also expected in view of the oxygen-rich atmosphere inferred from the AlO bands. However, the contribution from silicates to the SED is expected at longer wavelengths (Mason et al., 1998). On the whole however, there may be a dust component due to silicates, an additional component of cooler temperature dust which will not be seen in the near-IR JHK colors here and also more matter outside the dust shell -in the form of a molecular shell - as discussed shortly. Hence the dust mass derived here may be considered a lower limit.

Following the same approach as that for the dust shell, we derive the luminosity and radius of the source at the 2MASS epoch to be $L_\star \sim 0.3 L_\odot$ and $R_\star \sim 1.6 R_\odot$. The $T_{\rm eff}$ = 3250K is indicative of an early M type star. However $L_\star$ and $R_\star$ deviate considerably from those of a giant/supergiant and are closer to a main sequence star (for a M0V star, $L = 0.08 L_\odot$; $R = 0.6 R_\odot$). This is indicative that the star has possibly evolved to its pre-outburst state. It is puzzling that the 2MASS luminosity is lower than that of the dust shell seen presently. While the discrepancy is not large, it is expected that $L_{\rm dust}$ should be lower than $L_\star$ in case the dust is just reradiating the energy from the central source.

3.3. Modelling of the AlO bands and Discussion

It is difficult to locate the site of the AlO emission. Since the AlO bands are seen in emission they are not photospheric. Presumably it is mixed with the dust in the dust-shell or located outside it. The source of excitation of the bands is likely to be due to fluorescence by near-IR photons emitted from the star or from the dust shell (or both). We are attempting to model the AlO bands in details in a separate work. However, we present here a preliminary synthetic spectrum (Figure 1), computed for a vibrational and rotational temperature T(vib) = 3000K and T(rot)= 300K respectively. This spectrum gives a reasonable reproduction of the relative band strengths. The unrelated values of T(vib) and T(rot) indicate that the system is not in thermal equilibrium. The model calculations, done for the (1,0) and (2,0) bands, indicate a low rotational temperature in the range of 200-400K range is required to reproduce the observed AlO bands. This can be seen from Figure 3 where the (2,0) band profiles are shown for different values of T(rot).

Tsuji (1973) has calculated the molecular abundances of different species in physical conditions similar to cool stellar atmospheres. These calculations show that the production of AlO is highest in the temperature range 2000-2500K. It then reduces with decreasing temperature and by 1000K the abundance drops to 10^{-7} times its peak value. The above considerations indicate that AlO is produced at a site conducive for its generation i.e. the cool photosphere of V4332 Sgr where a temperature of 2300K prevailed shortly after the outburst. The generated AlO is subsequently lost, possibly in a wind, and is presently seen along with the dust shell. We rule out the possibility of AlO being created in the dust shell itself which is at too low a temperature (900K) for efficient AlO production. The same process of AlO production may also apply for V838 Mon where appropriate temperatures exist (Munari et al. 2002, Banerjee & Ashok 2002a; Crause et al. 2003). However an important distinction is that the AlO bands in V838 Mon are seen in absorption implying they are photospheric. They may appear in emission at a later stage. Tsuji's results (1973) show that AlH and AlOH (among other Al bearing molecules) may also be expected. However available data in the literature shows the AlH fundamental band lies at 6μm and the first overtone at 3μm i.e. outside the spectral coverage reported here (White et al., 1993; Deutsch et. al, 1987). For the AlOH isomer , there is only a theoretical paper (Hirota et al. 1993) where the O-H frequency is expected near 2.3μm. A laboratory confirmation of this should possibly be awaited before looking for such bands in the present data.

Although the outburst mechanism for V4332 Sgr/V838 Mon type of objects is not completely understood, available evidence indicates that the eruption is basically a dramatic expansion of the star into a supergiant accompanied by some mass loss in a moderate velocity wind (Bond et al. 2003). Here we have shown that the mass loss in such objects may continue

beyond the main eruption. Based on the present results on V4332 Sgr, it appears that post-outburst developments in these objects can be fairly rapid and interesting (e.g. the rich AlO spectra) and thus there is a need to monitor them regularly. A cold molecular environment can surround these stars in their post-outburst stage in sharp contrast to the extremely hot coronal gas in classical novae. Specifically in V4332 Sgr - given the predominace of AlO in the spectra - it would be worthwhile to look for the B-X band system of AlO in the optical and also for rotational transitions of the lower $X^2\Sigma^+$ levels in the sub-mm/mm region where several such lines are listed.

The research work at PRL is funded by the Department of Space, Government of India. We thank the UKIRT service program for observation time in the service mode and Chris J. Davis and Jane Buckle of UKIRT for doing the observations. UKIRT is operated by JAC, Hawaii, USA, on behalf of the UK Particle Physics and Astronomy Research Council.

REFERENCES

Banerjee, D.P.K., & Ashok, N.M., 2002a, A&A, 395, 161

Banerjee, D.P.K., & Ashok, N.M., 2002b, IAU Circ. 8036

Barnbaum, C., Omont, A., & Morris, M., 1996, A&A, 310, 250

Bernstein, L.S., Rudy, R.J., Lynch, D.K., Dimfl, W.L., Mazuk, S., Venturini, C.C., Puetter, R.C., & Perry, R.B., 2003, IAU Circ. 8082

Bond, H.E., Henden, A., Levay, Z.G., Panagia, N., Sparks, W.B., Starrfield, S., Wagner, R.M., Corradi, R.L.M., & Munari, U., 2003, Nature, 422, 405

Crause, L.A., Lawson, W.A., Warrick, A., Kilkenny, D., Van Wyk, F., Marang, F., & Jones, A.F., 2003, MNRAS, 341, 785

Deutsch, J.L., Neil, W.S., & Ramsay, D.A., 1987, J. Mol. Spectrosc., 125, 115

Geballe, T.R., Smalley, B., Evans, A. & Rushton M.T., 2002, IAU Circ. 8016

Hirota, F., Tanimoto, M., & Tokiwa, H., 1993, Chem. Phys. Letters, 208, 115

Koornneef, J., 1983, A&A, 128, 84

Launila, O., & Jonsson, J., 1994, J. Mol. Spectrosc., 168, 1

Martini, P., Wagner, R.M., Tomaney, A., Rich, R.M., Della Valle, M., & Hauschildt, P.H., 1999, AJ, 118, 1034

Mason, C.G., Gehrz, R.D., Woodward, C.E., Smilowitz, J.B., Hayward, T.L., & Houck, J.R., 1998, ApJ, 494, 783

Munari, U., Henden, A., Kiyota, S., Laney, D., Marang, F., Zwitter, T., Corradi, R.L.M., Desidera, S., Marrese, P., Giro, E., Boschi, F., & Schwartz, M.B., 2002, A&A, 389L, 51

Rich, R.M., Mould, J., Picard, A., Frogel, J.A., & Davies, R., 1989, ApJ, 341, L51

Soker, N., & Tylenda, R., 2003, ApJ, 582, L105

Tsuji, T., 1973, A&A, 23, 411

White, J.B., Dulick, M., & Bernath, P.F., 1993, J. Chem. Phys., 99, 8371

Woodward, C.E., Lawrence, G.F., Gehrz, R.D., Jones, T.J., Kobulnicky, H.A., Cole, J., Hodge, T., & Thronson (Jr.), H.A., 1993, ApJ, 408, L37

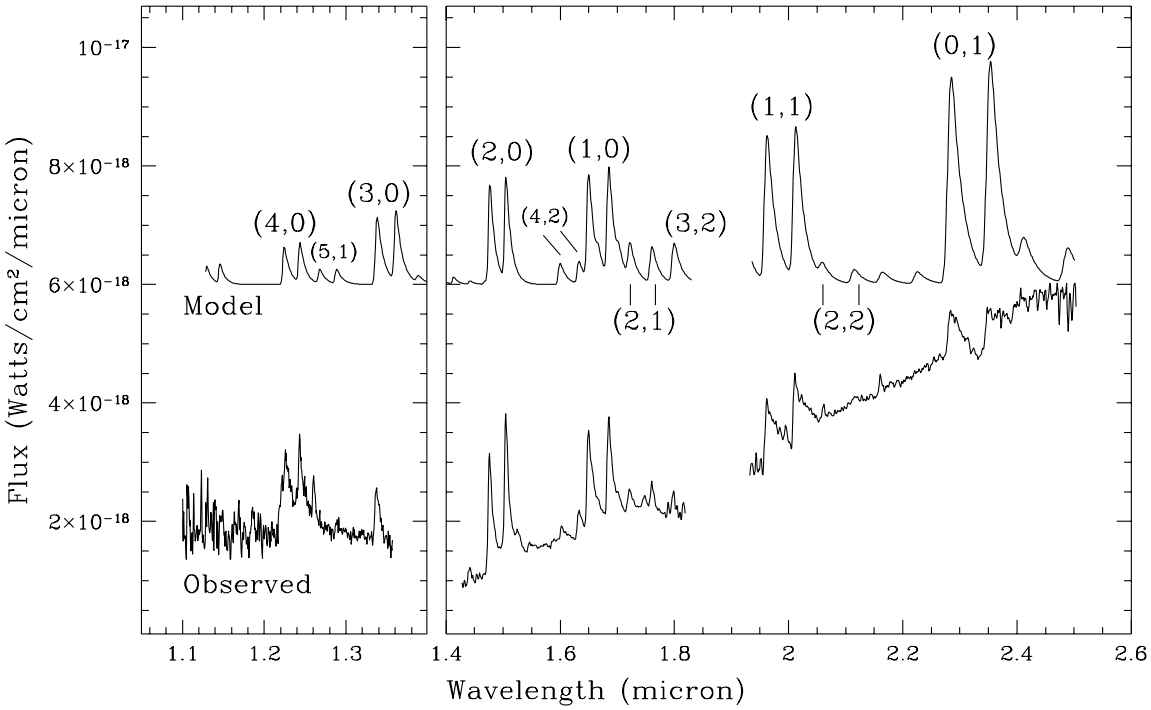

Fig. 1.— The observed JHK spectra of V4332 Sgr showing the prominent $A^2\Pi_i - X^2\Sigma^+$ emission bands of AlO are displayed in the bottom section. A computed, model spectrum is also shown in the upper half for comparison. The identifications of the detected bands are marked in the model spectrum.

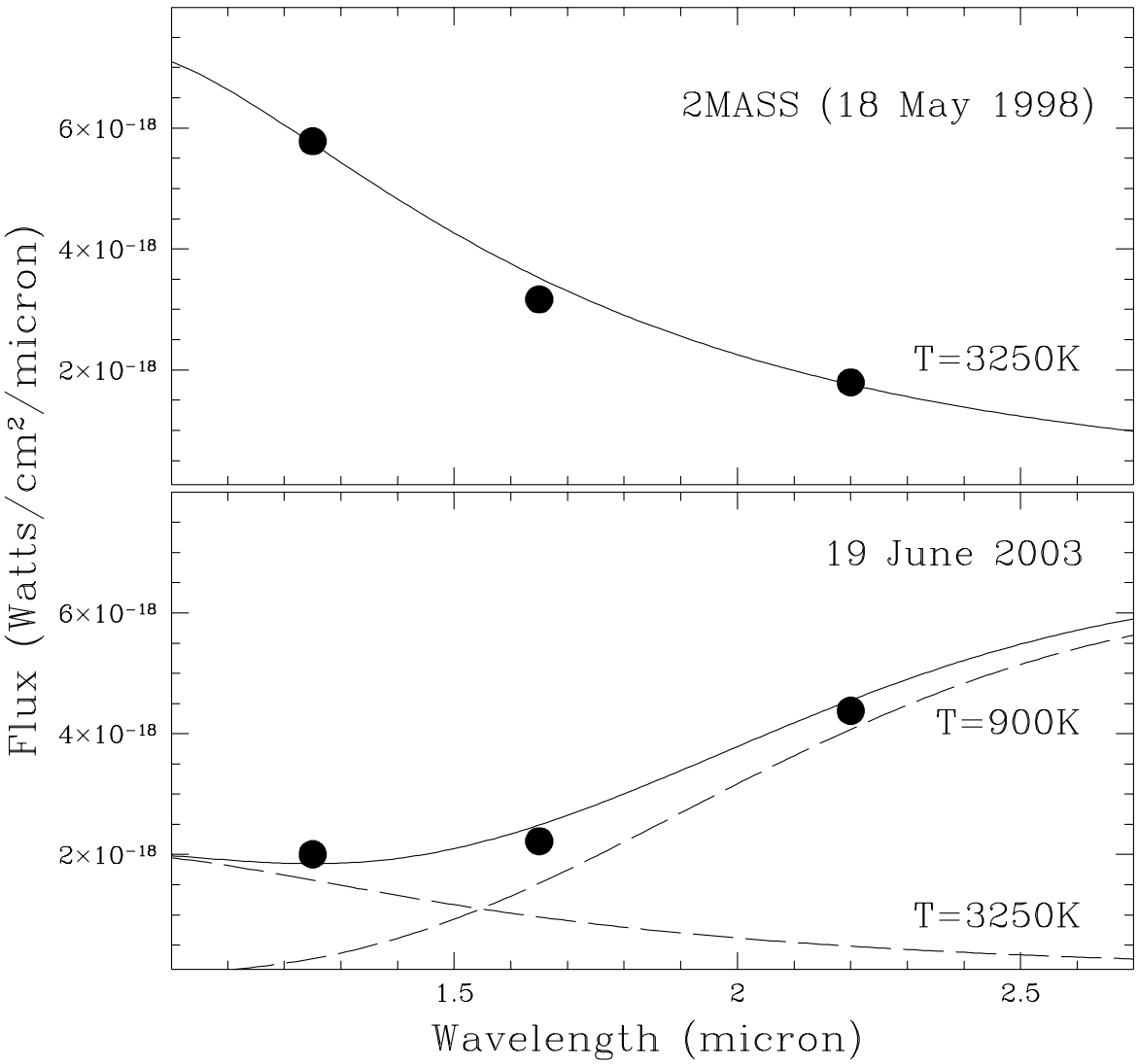

Fig. 2.— The top panel shows a T = 3250K black-body fit to the 2MASS data. The bottom panel, shows the sum (bold line) of 2 black-body componemts at T = 900K and 3250K respectively (dashed lines) fitted to the present JHK fluxes.

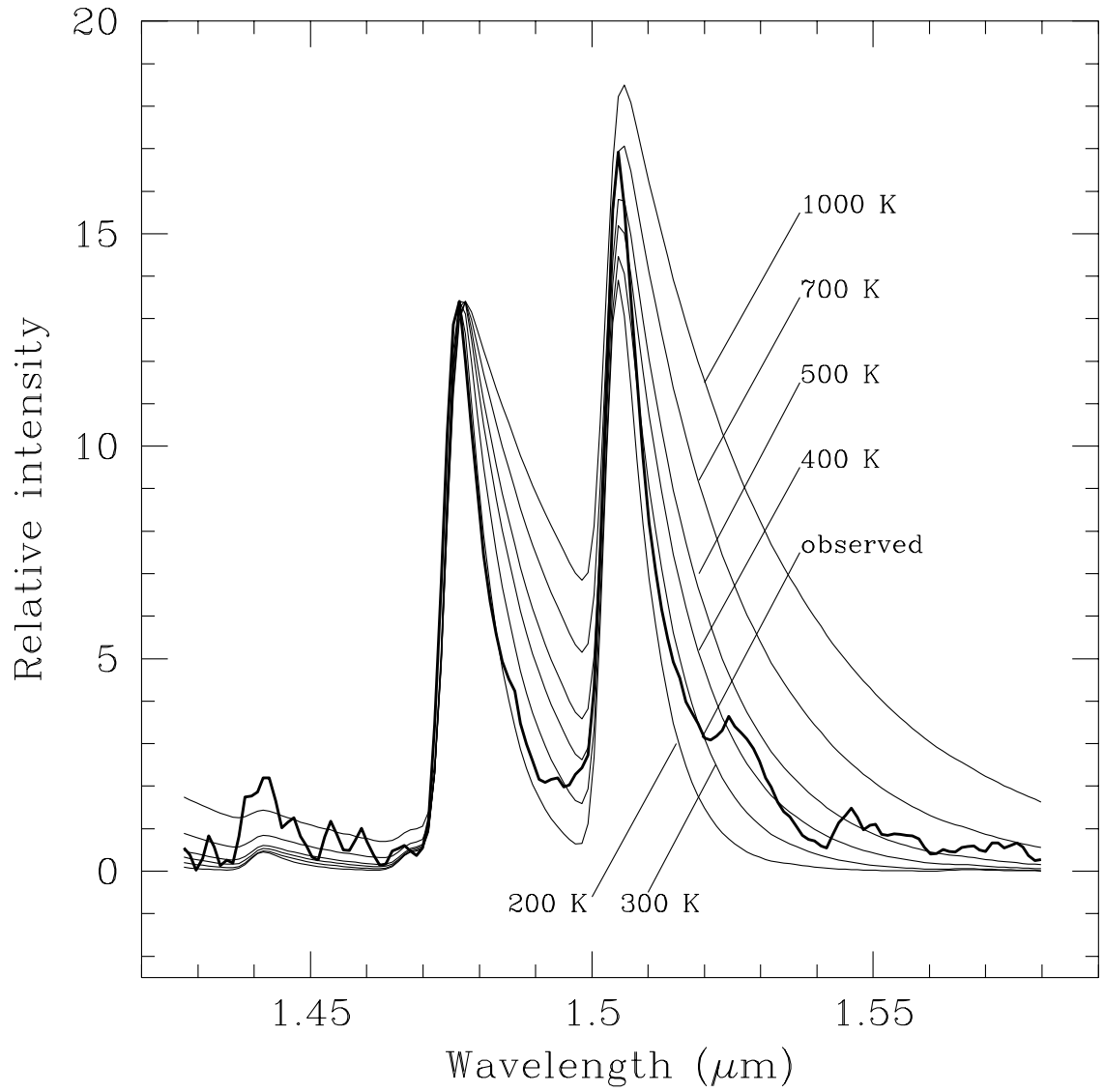

Fig. 3.— Model fits at different rotational temperatures for the (2,0) A-X band of AlO are shown. Please refer the text for further details.

Table 1: Log of spectroscopic observations

UT Date	UT	Grism	Resolution	Integration Time(s)
24 April 2004	13.879	HK	400-500	720
24 April 2004	14.319	Long J	2050	960
4 May 2003	14.902	IJ	300	1800

Table 2: Log of photometric observations for 19 June 2003

UT	Band	Exposure Time(s)	Integration Time(s)	Mag. (error)
12.199	J	50	250	13.251 (0.005)
12.017	H	10	90	11.986 (0.01)
11.955	K	4	80	10.023 (0.011)

Table 3: A list of the laboratory wavelengths for the $A^2\Pi_i - X^2\Sigma^+$ transitions of AlO

Band	$\lambda(\mu\text{m})$ $A^2\Pi_{3/2}$	$\lambda(\mu\text{m})$ $A^2\Pi_{1/2}$	Band	$\lambda(\mu\text{m})$ $A^2\Pi_{3/2}$	$\lambda(\mu\text{m})$ $A^2\Pi_{1/2}$
(1,0)	1.6837	1.6480	(1,1)	2.0106	1.9600
(2,0)	1.5035	1.4749	(2,1)	1.7589	1.7199
(3,0)	1.3589	1.3361	(5,1)	1.2874	1.2669
(4,0)	1.2425	1.2256	(3,2)	1.8409	1.7962
(0,1)	2.3514	2.2826	(4,2)	1.6311	1.6031